FINAL REPORT OF A PROJECT FUNDED BY THE EUROPEAN SCIENCE FOUNDATION (ORGANISOLAR PROGRAMME)

Nanocrystalline Metal Oxide/Polymer Hybrid Solar Cells: Device Preparation, Characterization and Investigation of Interfacial Electon-Transfer Processes (Exchange Grant 2533)

NOVEMBER 2009 – FEBRUARY 2010

Grantee: Dr. John Noel Clifford, Institute of Chemical Research of Catalonia (ICIQ), Tarragona, Spain.

Host Institution: IMO-IMOMEC, Hasselt University, Diepenbeek, Belgium.

1. Introduction

Organic Photovoltaic (OPV) solar cells have been under rigorous investigation in the last number of years and are expected to make a significant contribution to the renewable energy sector in the near future.[1] The key advantage of course is that such devices can be constructed from low cost materials making them rather attractive for commercialisation. Additionally, the possibility of making OPV devices using roll-to-roll processing techniques on flexible substrates makes them even more attractive from an economic standpoint. Several disadvantages persist however including low efficiency and poor stability.

The highest efficiencies (~ 6%) have been recorded using blends of fullerene C_{60} and a polymeric donor.[2, 3] In such systems the high electron affinity fullerene acceptor and polymer are mixed together in solution and deposited onto a conducting substrate forming a thin layer of what is referred to as a bulk heterojunction (BHJ). Film morphology can have a big effect on device efficiency with rough surfaces and the presence of voids increasing cell resistance and also the chance of short circuits. Another big problem is phase separation, which happens when the polymer and fullerene separate from one another, obviously resulting in a dramatic drop-off in cell efficiency.

In addition to fullerene derivatives, n-type inorganic materials such as II-VI compound semiconductors and metal oxides have been investigated as electron acceptors in polymer based devices due to their relatively high electron mobility, high electron affinity and good physical and chemical stability. Such devices are commonly referred to as "hybrid" solar cells. Hybrid BHJ devices based on polythiophene and CdSe have been reported with promising efficiencies of up to 2.6%.[4]

Hybrid BHJ cells based on nanocrystalline metal oxides can be formed from blends of metal oxide and polymer. However the metal oxide can also be in the form of a nanoporous film of nanoparticles that offers a much better defined pathway for electron transport to the back contact. The properties (electronic, electron transport, nanoparticle shape etc.) of nanocrystalline films of metal oxide semiconductors have been

intensively studied since the early 1990´s following on from advances in sol-gel chemistry and the development of the dye sensitized solar cell (DSSC).[5] TiO_2 in particular is attractive as it is a non-toxic low cost material which has a high electron affinity and high electron mobility. In addition, the surface chemistry of such materials is by now well understood allowing surface modification by small molecules and different dye sensitizing species. Hybrid devices based on blends have shown promising efficiencies (1.7% for TiO_2[6] and 1.6% for ZnO[7]). Devices based on porous nanocrystalline films with morphologies such as mesoporous structure and nanotube arrays have shown lower efficiencies (~ 1% utilizing TiO_2). An obvious problem concerning the use of nanocrytalline films in OPV devices remains how to successfully infiltrate the film pores with the polymer.

One way to increase the efficiency of hybrid BHJ is to immobilize a dye sensitizer species onto the surface of the metal oxide that can improve light harvesting of the incident radiation. A key difference between a hybrid BHJ utilizing a dye sensitizer and a DSSC utilizing a solid state electrolyte such as spiro-OMeTAD is that both the dye and the polymer in the hybrid BHJ can absorb light contributing to photocurrent whereas spiro-OMeTAD in ss-DSSC has no light absorbing function. Hybrid BHJ modified with dye sensitizers have shown rather disappointing increases in device efficiency, however recently Mor et al[8] showed cells with excellent efficiencies of 3.8% utilizing TiO_2 nanotube arrays and a red absorbing dye sensitizer.

2. Project Objective

Building upon the extensive experience of the Palomares group at ICIQ in the investigation of DSSC utilizing different dye sensitizer species and the Manca group at IMO-IMOMEC at making efficient BHJ devices the main objective of this project is to investigate hybrid BHJ devices incorporating several commercially available and novel dye sensitizers. The dye is expected to have several functions within the device including:

1) Passivate the hydrophilic surface of the metal oxide and help infiltration of the hydrophobic polymer into the pores of the nanocrystalline film.

2) Increase light harvesting and contribute to an increase in efficiency.

In particular, we want to investigate the effect of the different dye structures upon polymer infiltration into the porous film and also study the different charge transfer processes at the TiO_2/dye/polymer interface.

Several kinds of dye sensitizer are used in this project: Ruthenium polypyridals, phthalocyanines and an organic squarine dye. Their structures are shown in Scheme 1. Red absorbing dyes are of particular interest for use in BHJ devices as they absorb in the near-IR where P3HT and many other polymers absorb poorly.

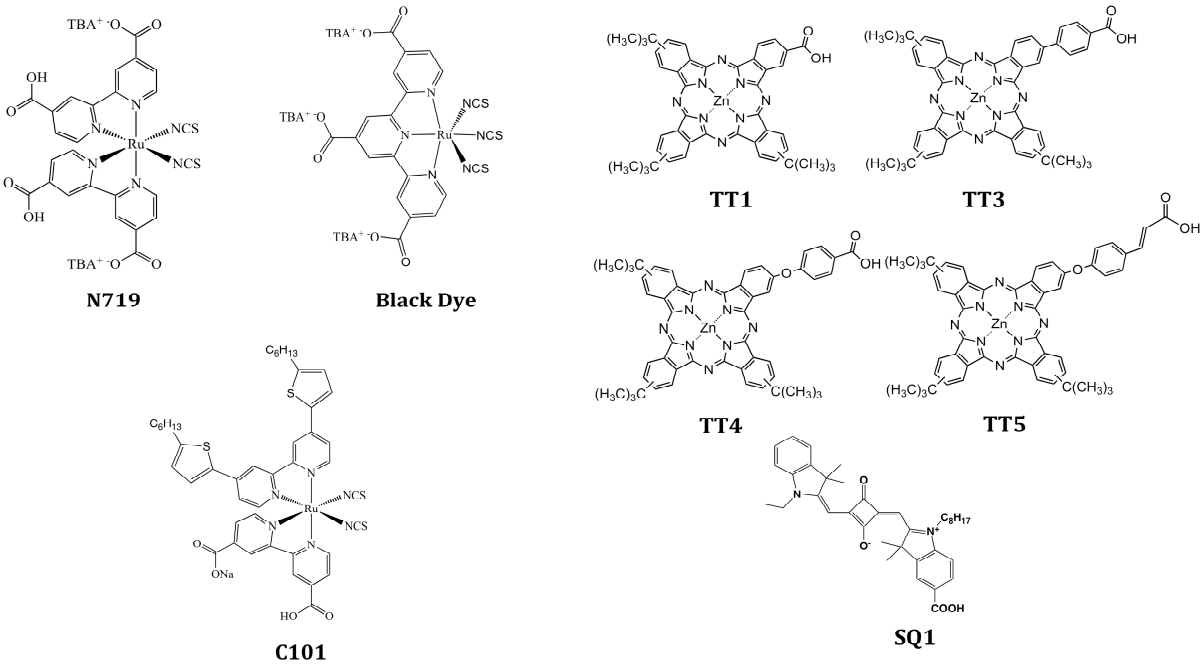

Scheme 1. Structures of the dyes used in this study.

3. Experimental

3.1 Sample Preparation

TiO_2 was used exclusively as the metal oxide semiconductor in this study. The TiO_2 paste (Solaronix) consisted of ~ 37 nm diameter nanoparticles. Regioregular P3HT (Reike) was used as the polymer. Dyes TT1, TT3, TT4 and TT5 were synthesised at the laboratory of Prof. Tomas Torres (Universidad Autónoma de Madrid).[9] SQ1 was supplied by Prof. Ko (Korea University). N719 and Black Dye were purchased from Solaronix. C101 was supplied by Prof. Palomares (ICIQ). After numerous trials with different metal contacts, different glass substrates (i.e. ITO v's FTO) and different dense TiO_2 layer thicknesses the optimized device geometry as shown in Scheme 2 was selected for this study.

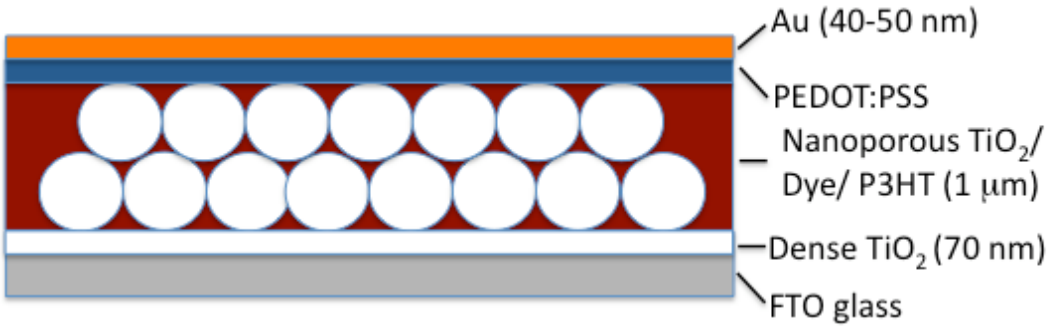

Scheme 2. Geometry of the solar cell devices used in this study.

3.1.1 Preparation of TiO_2 Photoelectrode

Photoelectrodes consisted of a double layer structure. Onto clean F-doped SnO_2 glass substrate (15 Ωsq^{-1}) a compact layer of dense TiO_2 of ~ 70 nm was deposited by spray pyrolysis followed by annealing at 450^oC for 20 mins. Onto this a second layer of ~ 1 μm nanocystalline TiO_2 was deposited by spin coating TiO_2 paste followed by annealing at 450^oC for 40 mins.

3.1.2 Dye sensitization of TiO_2 electrodes

TiO_2 electrodes were sensitized for either 4 or 15 hours in $5x10^{-5}$ M solutions of TT1, TT3, TT4, TT5 and SQ1 in ethanol and in $5x10^{-4}$ M solutions of N719, Black Dye and C101 also in ethanol. Additionally, all dye solutions except N719 contained Chenoxycholic Acid (10-30 mM) which is added to avoid dye aggregation on the surface of the TiO_2. Following sensitization the electrodes were removed from the dye solution, rinsed in ethanol and dried in air.

3.1.3 P3HT Deposition

P3HT was incorporated into the mesoporous TiO_2 electrode in the glove box under inert conditions. Firstly the electrode was dipped in a dilute P3HT solution (3 mg / ml) in chlorobenzene for 30 minutes. The electrode was then removed, allowed to dry and annealed at 50^oC for 10 mins. A second concentrated solution of P3HT (16mg / ml) was spin coated onto the electrodes and the samples were then annealed again at 100^oC for 10 mins.

3.1.4 PEDOS:PSS/Au Deposition

To complete the cell, a thin layer of PEDOT:PSS was spin coated onto the electrodes and the samples annealed at 120 ^oC for 10 minutes. Finally, 40-50 nm of gold was evaporated onto the sample as the metal contact. Each sample consisted of 4 diodes, two of 3 mm^2 and two of 5 mm^2.

3.2 Sample Characterization

3.2.1 Absorption Spectra

Device absorption spectra were measured using a double beam Cary 500 Scan UV-Vis-NIR Spectrophotometer.

3.2.2 I-V Characterization

The I–V characteristics were measured with an Oriel solar simulator equipped with a Xenon Short Arc lamp with a power of 150 W.

3.2.3 EQE Characterization

Fourier-Transform Photocurrent Spectroscopy (FTPS) is a very powerful technique, able to measure External Quantum Efficiency (EQE) and photocurrent spectra of photovoltaic devices over several orders of magnitude. In contrast to the classical monochromatic techniques, FTPS is a dispersive technique, meaning that the sample is illuminated by light of several photon energies simultaneously. The high sensitivity is sufficient to detect new absorption features below the optical gap of the investigated photovoltaic material. FTPS was only recently (2002) introduced as a fast characterization technique for solar cells by Vanecek et al.[10]

The simplest way to spectrally resolve a quantity is to illuminate a sample or photovoltaic device with monochromatic light, perform a measurement of the quantity, and then scan to the next wavelength. In order to obtain such a monochromatic light beam, a white light source is used to illuminate a diffraction grating that splits the white light into a rainbow of colors. With the aid of a slit, the desired wavelength is selected. With a band pass filter, higher order diffracted wavelengths are filtered out. Due to the size of the slit, the selection of photons of a single energy is not possible. A spectral band, of certain bandwidth, centered on the wavelength of interest is transmitted through the system. The spectral resolution $\Delta\lambda$ is proportional to the width of the slit. However, the total amount of power which passes through the monochromating system is also proportional to the slit width. The use of a monochromator thus results in an exchange between spectral resolution and signal to noise ratio. This can in particular be a problem when one would like to spectrally resolve very sharp peaks due to molecular vibrations or rotations in the infrared.

The dispersive technique, Fourier-transform infrared spectroscopy (FTIR), based on an interferometer instead of a monochromator, provides a solution to this problem. In this technique, a white light source illuminates a Michelson interferometer. In the interferometer, the light beam is split into two by a beam splitter. A path length difference $\delta=2d$ between the beams is created, before both beams are joined back together. The spectral resolution is set by the maximum path length difference δmax. Here a major advantage of the Fourier-transform technique becomes clear. It allows to measure at very fine spectral resolutions (down to 0.125 cm-1 for a δmax of 4 cm), while maintaining high signal to noise ratio.

4. Results

4.1 Absorption spectra

The absorbance spectra for complete devices made with the ruthenium polypyridal dyes N719, Black Dye and C101are shown in Figure 1 below where the TiO_2 electrodes have been sensitized in dye solutions for different times (4 and 15 hours).

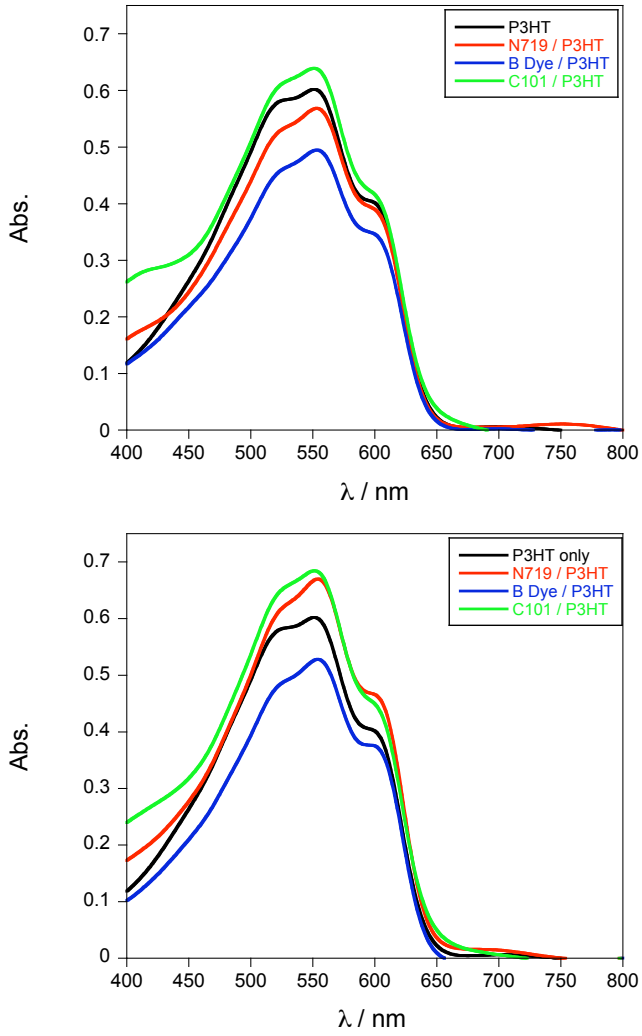

Figure 1. Absorption spectra of hybrid devices made without dye (P3HT only), N719, Black Dye and C101 where the TiO_2 electrode has been sensitized for 4 hours (top) and 15 hours (bottom).

The absorbance of P3HT is centred on a narrow band at around 550 nm. All of the ruthenium polypyridal dyes also show broad absorbance in this region however they contribute very little to the light absorbance of the electrode due to the low absorption

extinction coefficient of such dyes (13900 $M^{-1}cm^{-1}$ at 541 nm for N719)[11] in comparison to the conjugated P3HT polymer. It is apparent that the dye can have a big effect on the amount of polymer in the sample. When C101 is used to sensitize the TiO_2 more P3HT is present in the electrode when compared to when no dye is used. This may be due to the thiophenes on the pyridine ligands which could be orientated away from the TiO_2 surface when C101 is anchored to it and thus being able to interact with the hydrophobic P3HT polymer, drawing it into the pores of the film. It would appear that the Black Dye has the opposite effect, showing rather less P3HT infiltration compared to the samples made in the absence of a dye. This may be because when this dye is anchored to the TiO_2 surface the terpyridine are proximate to the TiO_2 surface with the polar NCS groups orientated away from the surface. N719 has little impact on the amount of P3HT infiltration in the sample.

The amount of time used for sensitization is found to have little impact on the amount of P3HT in the samples. This is presumably because the concentration of the dye on the TiO_2 surface has reached its maximum after 4 hours with longer sensitization times not leading to any significant increase in dye concentration on the electrode.

Figure 2 shows the spectra for devices made with the red absorbing dyes TT1, TT3, TT4, TT5 and SQ1 where the TiO_2 electrodes have been sensitized in dye solutions for different times (4 and 15 hours).

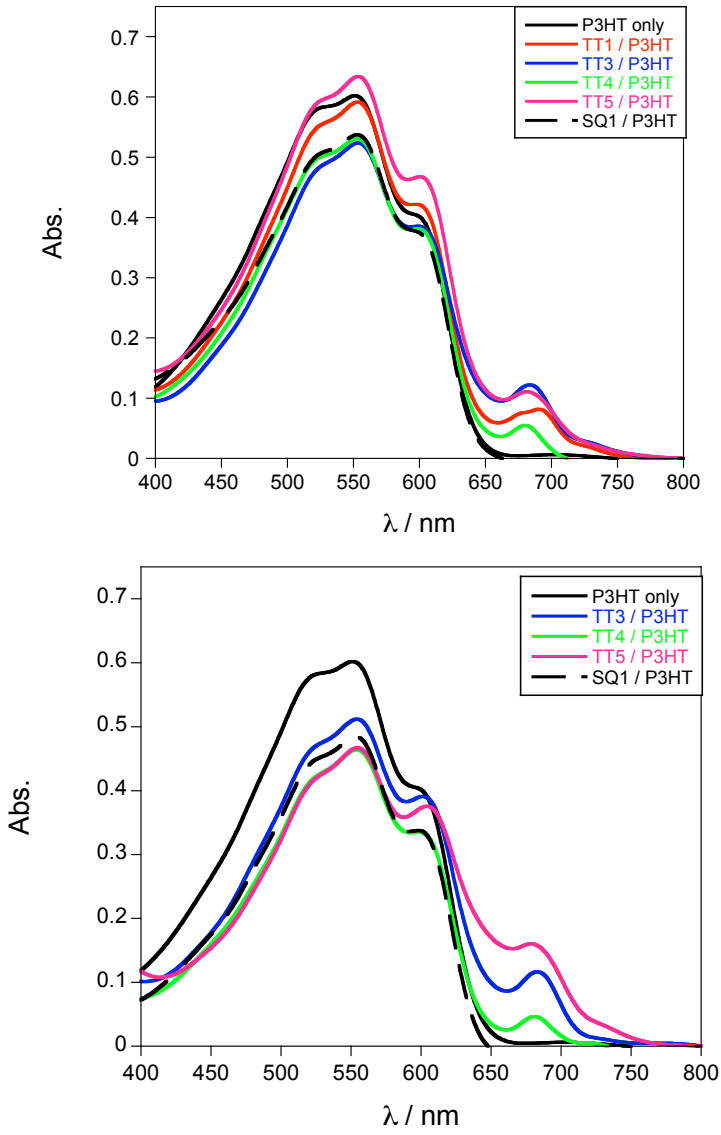

Figure 2. Absorbance spectra of hybrid devices made without dye (P3HT only), TT1, TT3, TT4, TT5 and SQ1 where the TiO_2 electrode has been sensitized for 4 hours (top) and 15 hours (bottom).

In addition to the P3HT band at 550 nm we can see the contribution of each of the phthalocyanine dyes at ~ 675 nm (the λ_{max} of SQ1 is ~ 650 nm and so masked by the P3HT absorbance). However, in the case of the devices made using TiO_2 electrodes sensitized for 4 hours, the presence of the dyes seems to have rather little effect on the amount of P3HT in the devices. This is rather surprising as the highly conjugated phthalocyanine systems and squarine SQ1 dye would be expected to interact well with the hydrophobic P3HT. Furthermore, if the sensitization time is increased to 15 hours even less P3HT is observed in the devices. Further investigations are currently underway to resolve the reasons behind these observations.

4.2 I-V Characterization

The I-V curves of the hybrid devices were recorded and are shown in Figure 3 below.

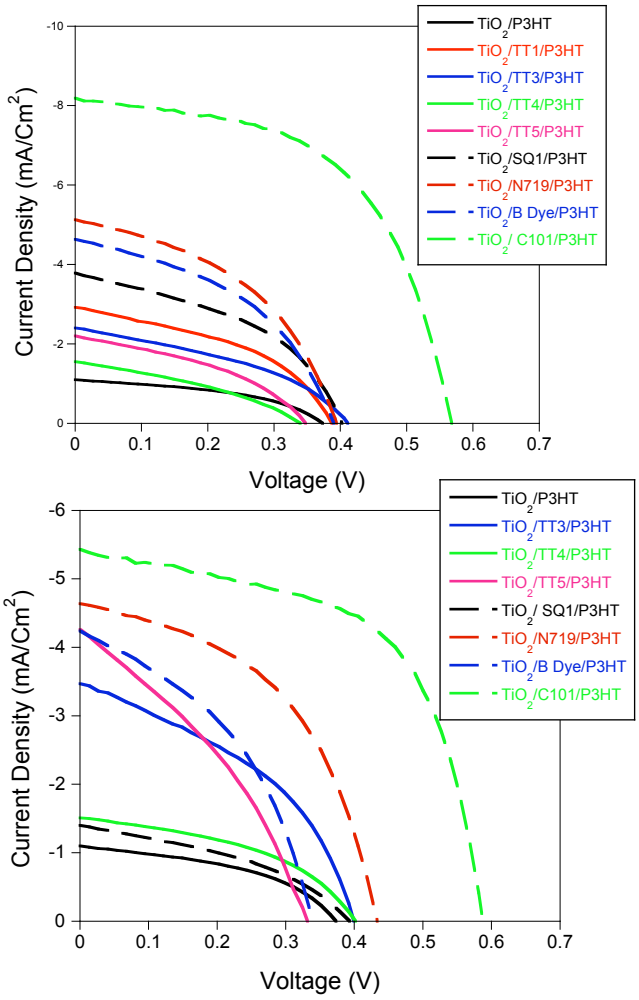

Figure 3. I-V curves of devices in the absence of dye and with the dyes N719, Black Dye, C101, TT1, TT3, TT4, TT5 and SQ1 where the TiO_2 electrode has been sensitized for 4 hours (top) and 15 hours (bottom).

The I-V data is also summarised in Table 1.

Table 1. I-V data of devices measured under AM 1.5 simulated solar radiation.

Device	J_{sc} (mA cm^{-2})	V_{oc} (V)	FF	η (%)*
TiO_2/P3HT	1.10	0.37	0.43	0.18 (0.09)
TiO_2/TT1/P3HT (4 hour sensitization)	2.92	0.39	0.42	0.48 (0.34)
TiO_2/TT1/P3HT (15 hour sensitization)‡	--	--	--	--
TiO_2/TT3/P3HT (4 hour sensitization)	2.40	0.40	0.39	0.38 (0.29)
TiO_2/TT3/P3HT (15 hour sensitization)	3.47	0.40	0.40	0.57 (0.41)
TiO_2/TT4/P3HT (4 hour sensitization)	1.55	0.33	0.35	0.18 (0.09)
TiO_2/TT4/P3HT (15 hour sensitization)	1.96	0.43	0.44	0.38 (0.31)
TiO_2/TT5/P3HT (4 hour sensitization)	2.20	0.35	0.38	0.30 (0.27)
TiO_2/TT5/P3HT (15 hour sensitization)	4.26	0.33	0.33	0.48 (0.29)
TiO_2/SQ1/P3HT (4 hour sensitization)	3.84	0.40	0.42	0.66 (0.29)
TiO_2/SQ1/P3HT (15 hour sensitization)	1.40	0.39	0.39	0.21 (0.14)
TiO_2/N719/P3HT (4 hour sensitization)	5.11	0.39	0.44	0.89 (0.75)
TiO_2/N719/P3HT (15 hour sensitization)	4.64	0.43	0.48	0.97 (0.81)
TiO_2/Black Dye/P3HT (4 hour sensitization)	4.63	0.39	0.43	0.79 (0.64)
TiO_2/Black Dye/P3HT (15 hour sensitization)	4.24	0.33	0.41	0.60 (0.49)
TiO_2/C101/P3HT (4 hour sensitization)	8.19	0.56	0.55	2.56 (2.08)
TiO_2/C101/P3HT (15 hour sensitization)	5.43	0.58	0.58	1.84 (1.50)

* The efficiency for the best diodes tested is given and the average of all of the working diodes for each sample is given in parenthesis.

‡Sample **TiO_2/TT1/P3HT** was destroyed during the spin coating of the P3HT polymer.

The presence of a dye incorporated into the hybrid devices can be seen in all cases to improve the device efficiency when compared to devices in which no dye is present. The increase in efficiency of the devices incorporating the red absorbing dyes we can presumably ascribe to the improved light harvesting of these devices. In the case of

devices made with the ruthenium polypyridal dyes, the improvement in the case of C101 may be ascribed to the improved infiltration of the P3HT into the pores of the TiO_2, however the improvement in efficiency of the devices made with N719 and Black Dye is more difficult to explain as these devices do not show improved P3HT infiltration. It may be because even though there is no actual increase in polymer content in these devices, there is much better interaction between the polymer and TiO_2 surface when a dye is present. Transient absorption spectroscopy can be utilized to gauge the amount of charge separation in these devices (see Future Work and Collaboration). The optimum sensitization time seems to be 15 hours for the phthalocyanine dyes and N719 whereas for SQ1, Black dye and C101 only 4 hours is necessary. A more thorough study investigating the effect of sensitization time upon device efficiency is necessary (see Future Work and Collaboration).

Devices made using C101 show the highest efficiency. The figure of 2.56% for a single diode is excellent when compared to similar studies in the literature on hybrid devices made using dyes. The difference in molecular structure between N719 and C101 is rather small but the effect on the efficiency of devices made using these sensitizers is quite large showing how subtle changes in molecular structure can have big effects upon efficiency.

4.3 EQE Characterization

FTPS was used to investigate the EQE of the hybrid devices. The EQE spectra for the reference device made without dye and with devices made from TT1, TT3, TT4, TT5, N719, Black Dye and C101 are shown below in Figure 4 where the TiO_2 electrode was sensitized for 4 hours. The data for devices where the TiO_2 electrode was sensitized for 15 hours has yet to be collected at IMO-IMOMEC due to technical problems with the FTPS system. Furthermore, the sample for SQ1 was found to have degraded during measurement and so is not shown.

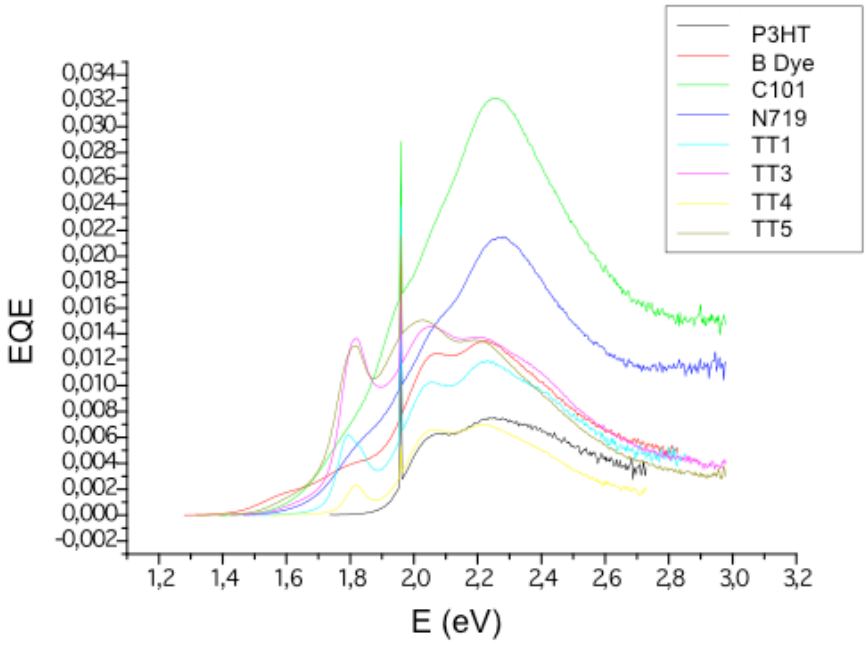

Figure 4. EQE spectra of devices in the absence of dye and with the dyes N719, Black Dye, C101, TT1, TT3, TT4, and TT5 where the TiO_2 electrode has been sensitized for 4 hours.

In the above spectra where the best sample shows an EQE of only 0.03 it is clear that the samples have degraded somewhat (these measurements were recorded after the I-V measurements described in the previous section). The above measurements were conducted in air at room temperature and perhaps these hybrid devices are not stable under such conditions. Repeated measurements on fresh devices measured in N_2 under glove box conditions shall be carried out shortly.

However in the above spectra we can see the contributions of the different light absorbing species (i.e. dye and/or polymer). The spectra for devices made using N719,

Black Dye and C101 display spectra quite similar to that of the reference sample made with P3HT only with a band centred at 2.2 eV (~ 550 nm). The devices made using red absorbing dyes TT1, TT3, TT4 and TT5 in addition to this band show a second band at lower energy centred at 1.8 eV (~ 675 nm) which is clearly the contribution of these dyes. These spectra clearly show that in the hybrid devices made using these red absorbing dyes the light harvesting has been improved towards the near-IR.

5. Conclusions

Hybrid solar cell devices based on films of nanocrystalline TiO_2, regioregular P3HT and several dye sensitizers including the ruthenium polypyridal dyes N719, Black Dye and C101 and a series of red absorbing phthalocyanine and squarine dyes have been investigated. C101 was seen to be the best dye for aiding polymer infiltration into the nanoporous film and we ascribe this to the thiophene units on its pyridine ligands which are orientated away from the TiO_2 surface thus being able to interact with the hydrophobic P3HT polymer, drawing it into the pores of the film. Devices made with the red absorbing dyes all show improved light harvesting. In all cases, devices made with dyes are superior in efficiency to the reference device made without any dye sensitizer. In particular, hybrid devices made with C101 show excellent efficiency of 2.56% for a single diode measured under AM 1.5 radiation.

6. Future Work and Collaboration

The work detailed in this report will be published in the near future. Further measurements will be conducted at the participating institutions on these hybrid devices. At IMO-IMOMEC hybrid devices will be made varying parameters such as the TiO_2 nanoparticle diameter, the nanoporous TiO_2 film thickness and the dye sensitization time. At ICIQ the charge transfer processes of these devices at the TiO_2/dye/P3HT interface using transient absorption spectroscopy (TAS) will be measured as well as the steady state luminescence lifetime of the dye and P3HT at this interface using time-correlated single photon spectroscopy (TC-SPC). Finally, capacitance and electron lifetimes in devices under operation mode shall be measured using photocurrent/photovoltage transient measurements.

Furthermore, the participating institutions have also planned to collaborate in other projects. It is planned to utilize some of the dye sensitizer species used in this study in BHJ devices using PCBM C_{60} and rr-P3HT. I-V and FTPS measurements will be conducted at IMO-IMOMEC and TAS, TC-SPC and photocurrent/photovoltage transient measurements will be undertaken in ICIQ.

7. References

(1) Clean Energy from Photovoltaics, Imperial College Press (London) 2001. Edited by Mary D. Archer and Robert Hill.

(2) Y. Liang, D. Feng, Y. Wu, S. T. Tsai, G. Li, C. Ray and L. Yu, *J. Am. Chem. Soc.* **2009**,131, 7792.

(3) A. B. Tamayo, X. D. Dang, B. Walker, J. Seo, T. Kent and T. Q. Nguyen, *Appl. Phys. Lett.* **2009**, 94, 103301.

(4) B. Q. Sun and N. C. Greenham, *Phys. Chem. Chem. Phys.* **2006**, 8, 3557.

(5) B. O´Regan and M. Grätzel, *Nature*, **1991**, 353, 737.

(6) Y. Y. Lin, T. H. Chu, C. W. Chen and W. F. Su, *Appl. Phys. Lett.* **2008**, 92, 053312.

(7) W. J. E. Beek, M. M. Wienk and R. A. J. Janssen, *Adv. Mat.* **2004**, 16, 1009.

(8) G. K. Mor, S. Kim, M. Paulose, O. K. Varghese, K. Shankar, J. Basham and C. A. Grimes, *Nano Lett.* **2009**, 9(12), 4250.

(9) J. J. Cid, M. García-Iglesias, J. H. Yum, A. Forneli, J. Albero, E. Martínez-Ferrero, P. Vázquez, M. Grätzel, M. K. Nazeeruddin, E. Palomares and T. Torres, *Chem. Eur. J.* **2009**, 15**,** 5130.

(10) M. Vanecek and A. Poruba, *Appl. Phys. Lett*. **2002**, 80, 719.

(11) M. K. Nazeeruddin, S. M. Zakeeruddin, R. Humphry-Baker, M. Jirousek, P. Liska, N. Vlachopoulos, V. Shklover, C.-H. Fischer and M. Graetzel, *Inorg. Chem.* **1999**, *38*, 6298.